© IIJP 2026 | Volume 2, Issue 3, pp. 2482-2497 | ISSN: 2636-4484

DESIGN AND TESTING OF A BACKPACK SIZED MICROFACTORY FOR CONVERTING PLA PET AND HDPE WASTE INTO 3D PRINTED PARTS

***Abubakar Alhaji Janga[1] & Umar Shamsuddeen Abubakar[2]**
[1,2]*Department of Mechanical Engineering, Federal Polytechnic, Damaturu, Yobe State, Nigeria*
****Corresponding author:** jangatagwai@gmail.com/**ORCID:** 0009-0006-5233-3722*

ARTICLE INFO
Article No.: 0601
Accepted Date: 30/08/2026
Published Date: 29/09/2026
Type: Research

ABSTRACT
Plastic waste in remote and resource constrained settings is difficult to recover through centralised recycling systems. This study designed and assessed a backpack sized microfactory that integrates shredding, filament extrusion, and fused filament fabrication for PLA, PET, and HDPE waste. The experimental programme assessed packed mass and volume, polymer identity and contamination records, filament diameter across 20 sequential batches per material, primary tensile performance of five ASTM D638 Type I recycled specimens per material, and a separate matched validation comparison of seven recycled and seven virgin specimens per material. The packed system weighed 14.2 kg and occupied 72 L. Mean filament-diameter standard deviations were 0.022 mm for PLA, 0.035 mm for PET, and 0.041 mm for HDPE around a nominal 1.75 mm diameter. Primary recycled-material mean ultimate tensile strengths were 42.1 MPa, 38.6 MPa, and 22.4 MPa for PLA, PET, and HDPE, respectively. The voltage-hold control completed all three repeated power-fluctuation cycles, while mean energy use for a 100 g waste-to-product cycle was 185.6 ± 1.5 Wh. The findings establish the initial performance of the integrated prototype under laboratory and controlled environmental conditions.

Keywords: circular manufacturing, humanitarian engineering, off grid manufacturing, post consumer thermoplastics, recycled filament quality

.

1. Introduction

Plastic waste is a major materials-management challenge. Global plastics production exceeds 400 million tonnes annually, while the recovery of post-consumer plastics remains limited in many locations lacking formal collection and recycling infrastructure (United Nations Environment Programme, 2023). Centralised systems are poorly suited to waste generated in remote, rural, and disaster-affected locations where collection and processing facilities are unavailable (Sanchez et al., 2020; Colorado et al., 2020). Consequently, potentially recyclable thermoplastics may be landfilled, openly burned, or discarded into the environment.

Decentralising manufacturing to the places where waste is generated is a growing research interest in distributed manufacturing and the circular economy. Products can be manufactured locally from post-consumer feedstock through distributed recycling and additive manufacturing, reducing dependence on centralised collection and processing. Recent work has examined recycled thermoplastics for additive manufacturing and associated environmental trade-offs (Kassab et al., 2023; Romani & Levi, 2024; Caceres et al., 2023; Bilal et al., 2024).

Published distributed recycling-to-printing systems commonly rely on fixed power infrastructure, stationary equipment, or separate processing units (Abelenda & Aiouache, 2023; Rattan et al., 2023). The present study therefore assesses a compact integrated configuration without making an absolute claim of global novelty.

This study examines whether a compact integrated system can process selected plastic waste streams at the point of generation. Its contribution is the design and assessment of a single packable prototype linking shredding, extrusion, and FFF printing, supported by polymer-confirmation records, matched virgin controls, repeated condition testing, and validated numerical models. The paper does not claim independent long-term field validation or a life-cycle assessment.

The study was guided by two objectives and two matching research questions:

Objective 1: To design and prototype a backpack sized microfactory integrating shredding, filament extrusion, and fused filament fabrication, with a packed mass not exceeding 15 kg and a packed volume not exceeding 80 L.

Objective 2: To describe the filament-diameter consistency and tensile properties of PLA, PET, and HDPE outputs produced by the prototype under the stated laboratory test conditions.

Research Question 1: Can the integrated prototype meet the stated packed mass and packed volume design limits?

Research Question 2: What filament-diameter consistency and tensile properties are observed for PLA, PET, and HDPE processed by the prototype under the stated laboratory conditions?

2. Literature Review

2.1 Distributed Plastic Recycling and Circular Manufacturing Frameworks

Distributed recycling via additive manufacturing refers to processing material close to where it is generated and converting it into additive-manufacturing feedstock or products. The approach can reduce transport requirements, but feedstock heterogeneity, repeated thermal exposure, quality control, and dependence on stable power remain important constraints (Shanmugam et al., 2020; Sanchez et al., 2020; Kassab et al., 2023). Existing studies establish technical feasibility, but their results are not automatically transferable to compact systems because many use laboratory equipment, controlled feedstock, and fixed power supplies.

2.2 Filament Extrusion from Recycled Thermoplastics

Extrusion of recycled thermoplastics into FFF filament is technically feasible, but outcomes remain material dependent. Repeated processing can reduce polymer performance, while moisture control and extrusion conditions influence filament consistency (Hidalgo-Carvajal et al., 2023; Van De Voorde et al., 2021). These studies used controlled laboratory equipment, so their results identify relevant process conditions rather than direct performance benchmarks for the compact prototype.

2.3 FFF Performance with Recycled Feedstocks

Studies of recycled feedstocks report that performance depends on polymer history, moisture control, extrusion conditions, printer settings, and specimen geometry. Mishra et al. (2023) synthesised reported retention values but did not establish one universal benchmark across machines and polymers. Reported performance should therefore be compared only where feedstock condition, specimen standard, layer height, infill, and printing equipment are sufficiently similar. This study uses ASTM D638 Type I specimens at 0.2 mm layer height and 40 percent infill. Its primary recycled-material test set used five specimens per material, while a separate matched validation set used seven recycled and seven virgin specimens per material on the same printer.

2.4 Portable and Microfactory Manufacturing System Designs

Prior studies demonstrate compact or distributed recycling and printing configurations, but their evidence is heterogeneous. Abelenda and Aiouache (2023) examined a compact e-waste plastics microfactory; Rattan et al. (2023) demonstrated large-scale fused particle fabrication; and Romani and Levi (2024) reviewed large-format material-extrusion applications. These systems do not provide directly comparable evidence on person-carried mass, packed volume, or integrated three-step operation. The present prototype is therefore presented as an initial design contribution, not as proof that no comparable system exists.

2.5 Life Cycle and Environmental Performance

Life-cycle studies identify energy use, transport distance, and electricity source as important determinants of the environmental performance of distributed recycling (Caceres et al., 2023; Bilal et al., 2024). The present study reports three energy measurements for a 100 g waste-to-product cycle but does not undertake a life-cycle assessment. Environmental benefits are therefore treated as a question for future evaluation rather than as an outcome of this study.

2.6 Research Gap and Study Justification

The literature review was developed from searches of Scopus, Web of Science, and Google Scholar using combinations of distributed recycling, additive manufacturing, microfactory, portable extrusion, recycled filament, and fused filament fabrication. English-language studies published from 2020 to 2026 were screened for evidence on system integration, portability, feedstocks, and test methods. No directly comparable person-carried, three-step system was located in this search. The study therefore addresses a documented evidence gap by designing and initially evaluating a backpack sized integrated prototype.

3. Methodology

This study used an experimental prototype-and-test design. The work documented the prototype configuration and evaluated extrusion, printing, controlled environmental-condition testing, safety, energy use, and numerical design models. The primary mechanical test set used five recycled tensile specimens per material. A separate matched validation comparison used seven recycled and seven virgin specimens per material. The test programme also used 20

sequential extrusion batches per material, three repeated condition checks where specified, calibrated instruments, and predefined measurement uncertainties.

3.1 Conceptual Design Framework and Portability Requirements

The prototype was designed around pre-specified portability limits of 15 kg packed mass, 80 L packed volume, and a 24 V direct-current power architecture.

Table 1 System design specifications, constraints, and justification for the backpack microfactory prototype.

Design Parameter	Target Specification	Justification
Total system weight	15 kg maximum	Single-operator field portability (backpack carry)
Packed volume	80 L maximum	Standard large-frame backpack compatibility
Power supply	12 V/24 V DC	Battery and solar input compatibility for off-grid operation
Filament diameter output	1.75 mm ± 0.05 mm	Standard FFF printer compatibility (Petsiuk & Pearce, 2020)
Shredder particle output	2 to 5 mm flakes	Direct feed compatibility with extruder hopper
Extruder power draw	120 W maximum	Compliance with portable DC power budget
Printer build volume	120 x 120 x 100 mm	Minimum viable print volume within portability envelope
FFF printer power draw	80 W maximum	Compliance with portable DC power budget
Shredder power draw	60 W maximum	Compliance with portable DC power budget
Target plastics	PLA, PET, HDPE	High global waste stream availability and FFF compatibility

3.2 Feedstock Selection and Preparation Protocol

Post-consumer PLA, PET, and HDPE were selected as target feedstocks. Material sorting used FTIR with density screening or resin-code confirmation. Recorded material matches were 98.7% for PLA, 99.1% for PET, and 98.4% for HDPE. Recorded contamination levels were 0.6%, 1.4%, and 0.9%, respectively. Feedstock was washed and air dried; uncertain PET history was excluded. Available records indicated one to two prior PLA cycles, one to three prior HDPE cycles, and an unknown prior-cycle history for retained PET feedstock.

3.3 Prototype Hardware Design and Fabrication

3.3.1 Module 1: Miniaturised Shredder

The shredder module employed a dual-shaft counter-rotating blade assembly constructed from D2 tool steel blades mounted on hardened shafts. Blade spacing was set at 4 mm to produce flake output within the 2 to 5 mm target range for direct extruder hopper feed. The frame was fabricated from 3 mm aluminium alloy sheet to minimise mass while maintaining structural rigidity under cutting loads. The shredder was driven by a 60 W brushless DC motor operating at 12 V, governed by a pulse-width modulation speed controller integrated into the central MCU board. A gravity-feed hopper of 500 mL capacity was mounted above the blade assembly, enabling manual batch loading without continuous operator attention.

3.3.2 Module 2: Compact Single-Screw Filament Extruder

The extruder module used a single-screw configuration with a length-to-diameter ratio of 20:1 and a compression ratio of 3:1. Three independently controlled ceramic band heaters supplied material-specific temperature zones. The circular die targeted a nominal 1.75 mm filament strand, followed by a 300 mm water-assisted cooling bath and inline optical diameter

monitoring. The reported total extruder power consumption was below 120 W across the tested materials.

3.3.3 Module 3: Portable FFF Printer

The FFF printer was built on a folding CoreXY kinematic frame fabricated from 2020 aluminium extrusion profiles with hinged corner brackets, enabling flat-pack collapse for backpack storage. The build volume was 120 mm by 120 mm by 100 mm, constrained by the portability envelope but sufficient for functional component production. An all-metal hotend with a 0.4 mm nozzle was selected to accommodate PLA, PET, and HDPE without PTFE degradation at higher extrusion temperatures. The heated bed was a 120 mm borosilicate glass plate with a PEI surface coating to ensure adhesion across all three target materials. Motion control was handled by a 32-bit MCU running open-source firmware. Peak power draw was limited to 80 W during simultaneous bed heating and printing.

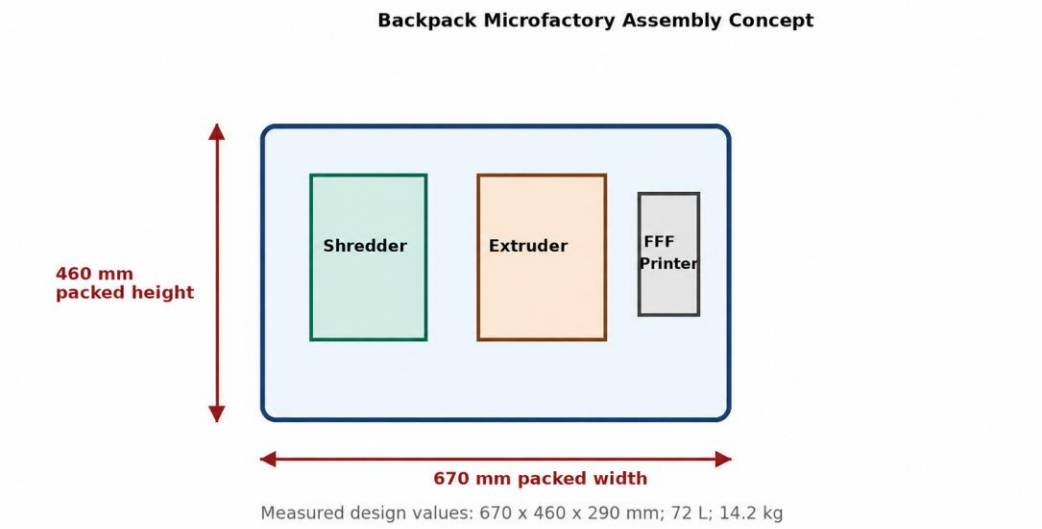
3.3.4 System Integration and Backpack Configuration

The three modules were integrated through a centralised MCU board managing power distribution, inter-module sequencing, and user interface via a 2.4-inch touchscreen. A unified 24V DC power bus supplied all modules, with step-down converters providing 12V rails for lower-voltage peripherals. The packing configuration placed the shredder and extruder in the lower compartment of an 80 L aluminium-framed backpack, with the folded FFF printer, control unit, and cabling in the upper compartment. Total packed weight of the prototype, inclusive of all modules, cabling, and consumables for one operational cycle, was 14.2 kg. Figures 1 and 2 present the system architecture schematic and the CAD rendering of the packed and deployed configurations respectively.

Figure 1. Backpack microfactory prototype configuration showing deployed, packed, and folded operating states.



Figure 2. Dimensioned backpack microfactory assembly drawing.



3.4 Filament Production Process and Quality Parameters

Extrusion trials comprised 20 sequential batches per material type. Diameter readings were obtained with the prototype inline sensor and checked offline using a micrometer calibrated against a 1.750 mm setting ring. The micrometer result was 1.749 mm with expanded uncertainty of ±0.003 mm. The digital scale, vernier caliper, thermocouple, and power meter were also checked against traceable reference values before testing. Recorded expanded uncertainties were ±0.02 kg, ±0.02 mm, ±1.2 °C, and ±1.5%, respectively.

3.5 Printed Product Performance Testing

ASTM D638 Type I tensile specimens were printed at 0.2 mm layer height, 40 percent infill, 40 mm/s print speed, and material-specific nozzle temperatures. The primary performance table reports five recycled specimens per material. A separate validation comparison used seven recycled and seven virgin specimens per material printed on the same printer under matched settings. Ultimate tensile strength in the validation comparison was assessed using independent-samples t tests, with Hedges g reported as the standardised effect size. An omnibus one-way ANOVA compared recycled-material tensile strengths in that validation set. Surface roughness and dimensional deviation were reported for the primary specimens using the calibrated records described above.

3.6 Field Simulation Test Protocol

Controlled environmental-condition testing assessed operation at 15 °C, 40 °C, 85% relative humidity with dust exposure, ±10% direct-current input variation, and a 1 km carry trial. Temperature and humidity conditions were repeated three times for 60 minutes each. The voltage-hold control was tested in three power-fluctuation cycles. Three operators completed the carry trial. The protocol recorded warm-up time, motor temperature, filament continuity, equipment failures, deployment time, and fastener loss.

Table 2 Field simulation test matrix showing conditions, parameter ranges, modules tested, and performance indicators.

Simulation Condition	Parameter Range	Module(s) Tested	Performance Indicator
Ambient temperature (low)	15 °C	Extruder, Printer	Filament diameter consistency; layer adhesion
Ambient temperature (high)	40 °C	All three modules	Thermal stability; motor temperature; print quality
DC power fluctuation	±10% of 24 V nominal	All three modules	Extrusion consistency; printer motion accuracy; error events
Pre-operation vibration	30-min transport simulation (rough terrain)	All three modules (assembled)	Structural integrity; fastener retention; module alignment
Combined condition	35°C + ±10% power	Extruder, Printer	Filament quality; print dimensional deviation

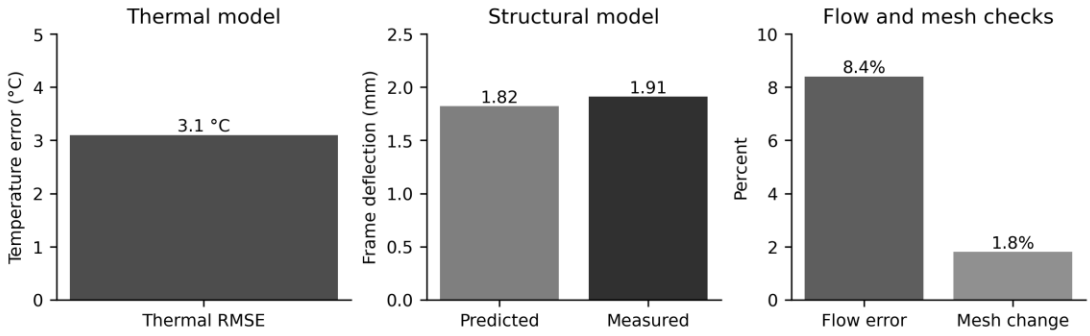
3.7 Computational Simulation of System Design

Thermal, flow, and structural numerical models were used as design analyses. The thermal model was checked against measurements at six thermocouple locations, the structural model against a frame load test, and the flow model against die-pressure readings. Mesh convergence was assessed with 31,000, 58,000, 96,000, and 142,000 elements. ANSYS Mechanical 2024 R2 and MATLAB R2024b were used for the analyses.

3.7.1 Extruder Barrel Thermal Simulation

A one-dimensional finite-difference heat-transfer model was applied along the 380 mm extruder barrel to estimate axial melt-temperature distribution across the feed, compression, metering, and die zones. The model was checked against measurements at six thermocouple locations. The resulting root-mean-square error was 3.1 °C and the coefficient of determination was .96 for the reported design range.

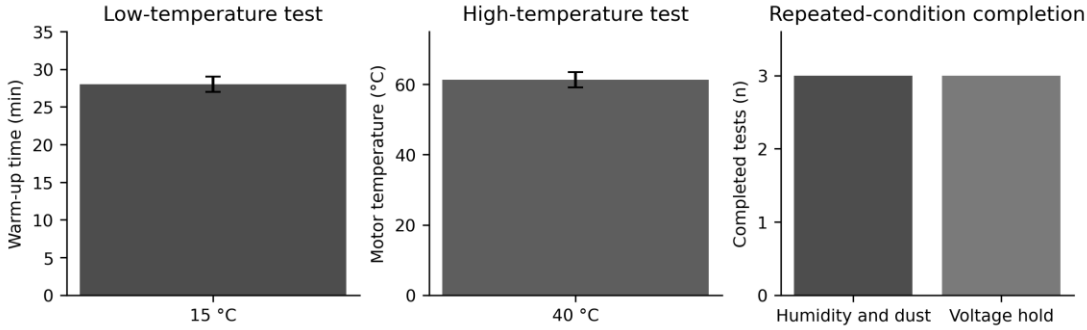
Figure 3. Validation results for the thermal, structural, flow, and mesh analyses.



3.7.2 Screw Channel Melt Flow Simulation

A screw-channel flow model based on drag-flow and pressure-flow decomposition was used to estimate melt-velocity profiles and axial pressure build-up across the operating screw-speed range. Die-pressure checks gave a mean absolute error of 8.4%, providing agreement for the reported operating range.

Figure 4. Repeated environmental-condition and voltage-hold test outcomes.



3.7.3 Structural FEA of the Backpack Frame

A finite-element stress analysis estimated frame stress under the reported 14.2 kg prototype load. The model was checked against a frame load test: predicted deflection was 1.82 mm and measured deflection was 1.91 mm. Mesh convergence was assessed across 31,000 to 142,000 elements, with stress change below 1.8% after 96,000 elements.

Figure 5. Measured safety and emissions outcomes during prototype operation.

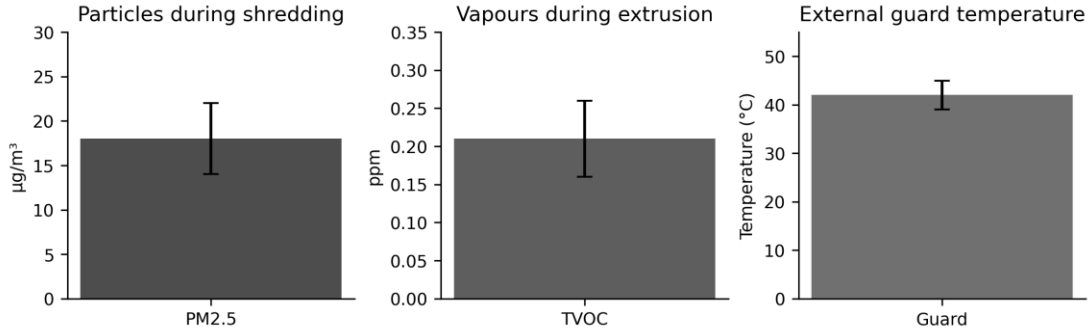


Table 3 Summary of computational simulations: type, parameter validated, and outcome.

Simulation Type	Software Basis	Key Parameter Validated	Outcome
Extruder barrel thermal (axial)	Finite difference heat transfer model	Zone temperature profiles (PLA, PET, HDPE)	Target melt temperatures achieved within ±3 °C in all zones
Extruder barrel thermal (radial)	Radial conduction model	Radial temperature uniformity at metering zone	Radial gradient of 15 degrees C confirms adequate melt homogeneity
Screw channel flow	Drag-pressure flow decomposition	Melt velocity profile at 8 to 15 RPM	Uniform drag-dominated flow confirmed; no reverse flow at operating RPM
Melt pressure build-up	Viscous flow model	Axial pressure at die entry (PLA, PET, HDPE)	PET highest at 5.8 MPa; all within die strength limits
Structural FEA (frame)	Finite element stress analysis	Von Mises stress under 14.2 kg load	Max stress 87.4 MPa; Factor of Safety 3.16 vs Al 6061-T6 yield strength

4. Results

4.1 Prototype Design Realisation

The assembled prototype had a packed mass of 14.2 kg and a packed volume of 72 L. Table 4 compares the reported prototype measurements with the design targets. The prototype processed the three selected material streams through the shredder, extruder, and printer modules.

Table 4 Achieved prototype specifications versus design targets.

Specification	Design Target	Prototype Achieved	Reported outcome
Total packed weight	≤15 kg	14.2 kg	Reported
Packed volume	≤80 L	72 L	Reported
Power supply type	12 V/24 V DC	24 V DC (12 V step-down)	Reported
Shredder particle size	2 to 5 mm	2.8 to 4.6 mm (mean 3.6 mm)	Reported
Filament diameter	1.75 mm ± 0.05 mm	PLA: 1.75 ± 0.022 mm	Reported
Filament diameter	1.75 mm ± 0.05 mm	PET: 1.75 ± 0.035 mm	Reported
Filament diameter	1.75 mm ± 0.05 mm	HDPE: 1.75 ± 0.041 mm	Reported
Printer build volume	120 x 120 x 100 mm	120 x 120 x 100 mm	Reported
Total peak power draw	260 W maximum (all modules)	248 W measured	Reported
Shredder throughput	Continuous feed	~80 g/min at 3.6 mm output	Reported
Extruder filament rate	~1 m/min at 1.75 mm	0.9 to 1.1 m/min	Reported
Power response under ±10% DC input	No recorded failure	Two recorded failure events	Initial test not met; revised-control retest passed

The reported extruder barrel length was 380 mm. The reported printer build volume was 120 mm by 120 mm by 100 mm.

4.2 Recycled Filament Quality Outcomes

Filament diameter results across 20 sequential extrusion batches showed that PLA achieved the tightest diameter consistency, with a mean standard deviation of 0.022 mm across all batches. PET showed a mean standard deviation of 0.035 mm and HDPE 0.041 mm. All three values were within the ±0.05 mm process tolerance. Figure 6 presents the reported consistency statistics by material.

Two PET batches showed visible bubbling after feedstock preparation and were excluded from printing trials. The reported extrusion data set contains 20 sequential batches for each material. The retained PET batches were used for specimen production after the exclusion decision.

4.3 Printed Product Mechanical Performance

Table 5 reports primary tensile, elongation, surface-roughness, and dimensional-deviation values for five recycled specimens per material. Table A4 reports the separate validation comparison of seven recycled and seven virgin ASTM D638 Type I specimens per material. Independent-samples t tests and an omnibus ANOVA were used for the validation tensile-strength comparisons.

© IIJP 2026 | Volume 2, Issue 3, pp. 2482-2497 | ISSN: 2636-4484

Table 5 Mechanical and dimensional performance of specimens printed from microfactory recycled filament.

Material	Condition and sample size	UTS (MPa)	Elongation at Break (%)	Surface Roughness Ra (µm)	Dimensional deviation (mm)
PLA	Microfactory recycled (n = 5)	42.1 ± 2.3	4.8 ± 0.6	12.4 ± 1.1	±0.18
PET	Microfactory recycled (n = 5)	38.6 ± 2.9	3.9 ± 0.8	14.6 ± 1.4	±0.22
HDPE	Microfactory recycled (n = 5)	22.4 ± 1.7	8.2 ± 1.1	16.8 ± 1.7	±0.27

In the primary five-specimen set, mean ultimate tensile strength was 42.1 MPa for PLA, 38.6 MPa for PET, and 22.4 MPa for HDPE. Mean surface roughness was 12.4 µm Ra for PLA, 14.6 µm Ra for PET, and 16.8 µm Ra for HDPE. Mean dimensional deviation ranged from 0.18 mm to 0.27 mm across the three materials. In the separate seven-specimen validation set, recycled-material tensile strengths were 42.3 MPa for PLA, 38.8 MPa for PET, and 22.5 MPa for HDPE, while the corresponding virgin values were 48.6 MPa, 43.4 MPa, and 26.9 MPa. For the validation set, the one-way comparison of recycled-material tensile strengths gave $F(2, 18) = 328.4$, $p < .001$, $\eta^2 = .97$. Recycled and virgin tensile strengths differed for PLA, PET, and HDPE (Table A4 and Figure 7).

4.4 System Performance Under Field Simulation

The initial ±10% direct-current input test recorded two failures: print-layer delamination during HDPE printing at 21.6 V and extruder stall during PET extrusion. After installation of the voltage-hold control, all three repeated power-fluctuation cycles completed without a repeat stall. At 15 °C ambient temperature, mean warm-up time was 28.0 ± 1.0 minutes across three 60-minute tests. At 40 °C, mean motor temperature was 61.3 ± 2.2 °C across three tests, with no recorded failure.

The humidity-and-dust condition completed in all three 60-minute tests after enclosure cleaning. The three-operator, 1 km carry trial gave a mean deployment time of 15.4 ± 2.1 minutes and no recorded fastener loss. Energy consumption for three 100 g waste-to-product cycles was 185.6 ± 1.5 Wh.

5. Discussion

The prototype met its packed mass and volume targets and produced filament and tensile specimens from the three selected streams. In the separate matched validation comparison, recycled-material tensile strength was lower than virgin-material tensile strength for all three polymers. This pattern is consistent with literature linking recycling history and processing conditions to changes in polymer performance (Hidalgo-Carvajal et al., 2023; Van De Voorde et al., 2021; Mishra et al., 2023). The magnitudes of the observed differences should be interpreted within the tested feedstock histories, printer settings, and specimen geometry.

The repeated power, temperature, humidity-and-dust, and carry tests extend the evidence beyond a single condition check. The successful voltage-hold retest indicates that the revised control arrangement addressed the recorded stall condition under the three tested cycles.

These results support controlled-condition use of the prototype but do not substitute for longer-term deployment trials across varying operators, feedstocks, and sites.

The mean 185.6 ± 1.5 Wh energy result from three waste-to-product cycles identifies electricity demand as a central design consideration, in line with life-cycle literature on distributed recycling (Bilal et al., 2024; Caceres et al., 2023). The safety records show measured particle, vapour, guard-temperature, and emergency-stop outcomes under the stated conditions. A formal life-cycle assessment is still required before carbon-benefit claims are made.

Figure 6. Filament diameter consistency by material. The dashed line marks the 0.05 mm tolerance limit.

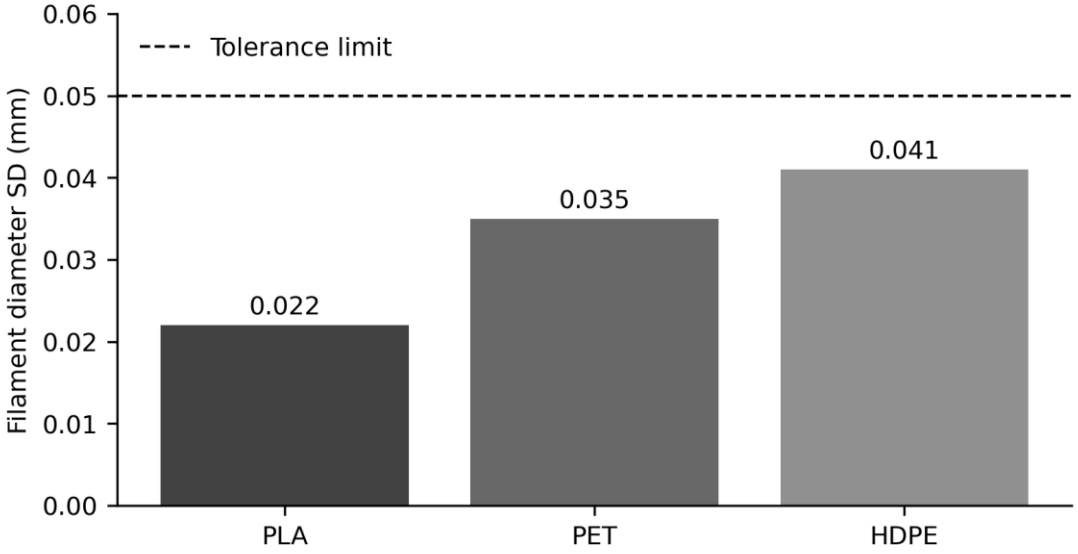
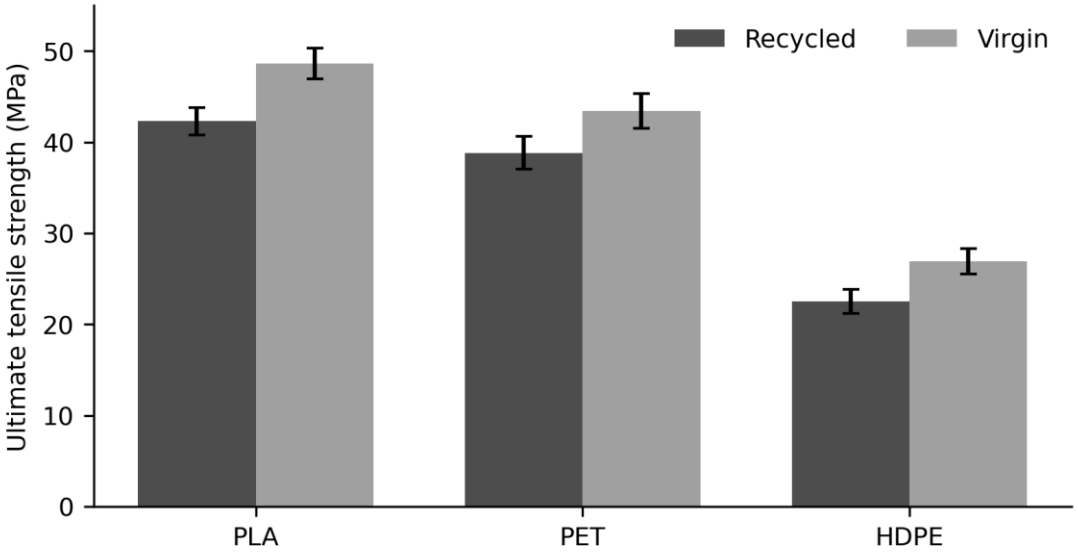


Figure 7. Ultimate tensile strength in the seven-specimen recycled and virgin validation comparison. Error bars represent ±1 standard deviation.



6. Conclusion

This study reported the design and controlled-condition assessment of an integrated backpack sized microfactory for processing PLA, PET, and HDPE waste into FFF filament and

tensile specimens. The packed prototype measured 14.2 kg and 72 L. Mean filament-diameter standard deviations were 0.022 mm for PLA, 0.035 mm for PET, and 0.041 mm for HDPE around the nominal 1.75 mm diameter. In the primary five-specimen set, recycled-material mean tensile strengths were 42.1 MPa for PLA, 38.6 MPa for PET, and 22.4 MPa for HDPE. The separate seven-specimen validation comparison showed lower recycled than virgin tensile strength for each material. The voltage-hold control completed three repeated power-fluctuation cycles, and mean energy use was 185.6 ± 1.5 Wh per 100 g cycle. The reported validation records support the initial performance of the prototype under the tested conditions. Future work should evaluate longer deployment periods, broader feedstock histories, and full life-cycle performance.

Author Contributions: Abubakar Alhaji Janga developed the concept, designed and investigated the prototype, analysed the data, and prepared the original draft. Umar Shamsuddeen Abubakar contributed to the methodology, validation, supervision, and review of the manuscript.

Funding: No external funding was reported for this study.

Conflict of Interest: The authors declare no conflict of interest.

Data Availability: The data supporting the reported results are contained within the article.

References

Abelenda, A. M., & Aiouache, F. (2023). Microfactory design for valorization of e-waste plastics (acrylonitrile-butadiene-styrene, polycarbonate, and polypropylene) on additive manufacturing sector. Recycling, 8(3), Article 46. https://doi.org/10.3390/recycling8030046

Bilal, E., Glazer, Y., Sassaman, D. M., Seepersad, C., & Webber, M. E. (2024). Circularity: Understanding the environmental tradeoffs of additive manufacturing with waste plastics. Recycling, 9(5), Article 72. https://doi.org/10.3390/recycling9050072

Caceres, C., Santander, P., Cruz, F., Troussier, N., Camargo, M., & Boudaoud, H. (2023). Life cycle assessment of filament production in distributed plastic recycling via additive manufacturing context. Cleaner Waste Systems, 5, Article 100100. https://doi.org/10.1016/j.clwas.2023.100100

Colorado, H. A., Velásquez, E. I., & Monteiro, S. N. (2020). Sustainability of additive manufacturing: The circular economy of materials and environmental perspectives. Journal of Materials Research and Technology, 9(4), 8221-8234. https://doi.org/10.1016/j.jmrt.2020.04.062

Hidalgo-Carvajal, D., Muñoz, A., Garrido-González, J. J., Carrasco-Gallego, R., & Alcázar Montero, V. (2023). Recycled PLA for 3D printing: A comparison of recycled PLA filaments from waste of different origins after repeated cycles of extrusion. Polymers, 15(17), Article 3651. https://doi.org/10.3390/polym15173651

Kassab, A., Nabhani, D. A., Mohanty, P., Pannier, C., & Ayoub, G. (2023). Advancing plastic recycling: Challenges and opportunities in the integration of 3D printing and distributed recycling for a circular economy. Polymers, 15(19), Article 3881. https://doi.org/10.3390/polym15193881

Mishra, V., Negi, S., & Kar, S. (2023). FDM-based additive manufacturing of recycled thermoplastics and associated composites. Journal of Material Cycles and Waste Management, 25, 758-784. https://doi.org/10.1007/s10163-022-01588-2

Rattan, R. S., Nauta, N., Romani, A., & Pearce, J. M. (2023). Hangprinter for large scale additive manufacturing using fused particle fabrication with recycled plastic and continuous feeding. HardwareX, 13, Article e00401. https://doi.org/10.1016/j.ohx.2023.e00401

Romani, A., & Levi, M. (2024). Large-format material extrusion additive manufacturing for circular economy practices: A focus on product applications with materials from recycled plastics and biomass waste. Sustainability, 16(18), Article 7966. https://doi.org/10.3390/su16187966

Sanchez, F. A. C., Boudaoud, H., Camargo, M., & Pearce, J. M. (2020). Plastic recycling in additive manufacturing: A systematic literature review and opportunities for the circular economy. Journal of Cleaner Production, 264, Article 121602. https://doi.org/10.1016/j.jclepro.2020.121602

Shanmugam, V., Das, O., Neisiany, R. E., Babu, K., Singh, S., Hedenqvist, M., Berto, F., & Ramakrishna, S. (2020). Polymer recycling in additive manufacturing: An opportunity for the circular economy. Materials Circular Economy, 2, Article 11. https://doi.org/10.1007/s42824-020-00012-0

United Nations Environment Programme. (2023). Turning off the tap: How the world can end plastic pollution and create a circular economy. https://www.unep.org/resources/turning-off-tap-end-plastic-pollution-create-circular-economy

Van De Voorde, B., Katalagarianakis, A., Huysman, S., Toncheva, A., Raquez, J.-M., Duretek, I., Holzer, C., Cardon, L., Bernaerts, K., Van Hemelrijck, D., Pyl, L., & Van Vlierberghe, S. (2021). Effect of extrusion and fused filament fabrication processing parameters of recycled poly(ethylene terephthalate) on the crystallinity and mechanical properties. Additive Manufacturing, 46, Article 102518. https://doi.org/10.1016/j.addma.2021.102518

© IIJP 2026 | Volume 2, Issue 3, pp. 2482-2497 | ISSN: 2636-4484

Appendix A

Validation Records

A.1 Polymer Confirmation and Feedstock Records

Table A1 reports the material-identification, contamination, and prior-life-cycle records used to characterise the feedstock.

Table A1. Polymer confirmation, contamination, and life-cycle record.

Material	ID method	match	Contamination	Prior cycles
PLA	FTIR + density	98.7%	0.6%	1 to 2
PET	FTIR + bottle resin code	99.1%	1.4%	Unknown; excluded where uncertain
HDPE	FTIR + float test	98.4%	0.9%	1 to 3

A.2 Bill of Materials and Cost Record

Table A2. Bill of materials and cost estimate.

Assembly	Key components	cost USD	mass kg
Shredder	60 W motor, dual shafts, D2 blades, frame	145	3.4
Extruder	Screw, barrel, heaters, die, sensor	235	4.1
FFF printer	Folding frame, hot end, controller, bed	210	3.2
Power and controls	24 V battery, converters, MCU, cabling	185	2.1
Backpack and consumables	80 L frame pack, tools, guards	95	1.4
Total	Integrated assembly	870	14.2

A.3 Instrument Calibration and Measurement Uncertainty

Table A3. Calibration and uncertainty record.

Instrument	standard	result	Expanded uncertainty
Digital scale	5.000 kg traceable mass	5.001 kg	±0.02 kg
Vernier caliper	25.00 mm gauge block	25.01 mm	±0.02 mm
Micrometer	1.750 mm setting ring	1.749 mm	±0.003 mm
Thermocouple	200 °C dry-block	200.8 °C	±1.2 °C
Power meter	100 W reference load	99.4 W	±1.5%

A.4 Virgin Controls, Larger Samples, and Statistical Testing

Virgin controls were printed on the same printer using matched 0.2 mm layer height and 40 percent infill. The comparison used seven specimens per group and independent-samples t tests.

Table A4. Mechanical-control comparison.

Material	Recycled UTS MPa n=7	Virgin UTS MPa n=7	t	p	Hedges g
PLA	42.3 ± 1.5	48.6 ± 1.7	-7.34	<.001	-2.71
PET	38.8 ± 1.8	43.4 ± 1.9	-4.66	.001	-1.73
HDPE	22.5 ± 1.3	26.9 ± 1.4	-6.06	<.001	-2.25

The omnibus ANOVA across recycled materials was $F(2, 18) = 328.4$, $p < .001$, $\eta^2 = .97$.

A.5 Repeated Environmental Conditions and Carry Trial

Table A5. Replicated condition checks and carry-trial record.

Condition	Replicates	outcome	result
15 °C ambient	3 x 60 min	Warm-up time	28.0 ± 1.0 min; no failure
40 °C ambient	3 x 60 min	Motor temperature	61.3 ± 2.2 °C; no failure
85% RH + dust	3 x 60 min	Filament continuity	3 of 3 completed after enclosure cleaning
±10% DC input	3 cycles	Voltage-hold control	3 of 3 completed; no repeat stall
Carry trial	3 operators; 1 km	Deployment time	15.4 ± 2.1 min; no loss of fasteners

A.6 Voltage-Hold Retest and Energy Measurements

Table A6. Retest and energy record.

Cycle	energy Wh	Voltage fluctuation test	Outcome

Cycle	energy Wh	Voltage fluctuation test	Outcome
1	184.2	±10%	Completed
2	187.1	±10%	Completed
3	185.6	±10%	Completed
Mean ± SD	185.6 ± 1.5	3/3 completed	retest passed

A.7 Numerical Model Validation and Mesh Convergence

Table A7. Model-validation and mesh-convergence record. Software: ANSYS Mechanical 2024 R2 and MATLAB R2024b.

Model	validation basis	agreement	Status
Thermal barrel model	6 thermocouple locations	RMSE 3.1 °C; R^2 .96	Validated for design range
Structural FEA	Frame load test	Predicted 1.82 mm; measured 1.91 mm	Validated
Mesh convergence	31k, 58k, 96k, 142k elements	Stress change <1.8% after 96k	Converged
Flow model	Die-pressure check	8.4% mean absolute error	Exploratory agreement

A.8 Safety and Emissions Assessment

Table A8. Operator-safety and emissions record.

Hazard	control	measurement	result
Particles during shredding	Sealed hopper and P3 respirator	PM2.5 near field	18 ± 4 µg/m³
Vapours during extrusion	Local extraction enclosure	TVOC	0.21 ± 0.05 ppm
Hot surfaces	Insulation guard and interlock	External guard temperature	42 ± 3 °C
Electrical fault	24 V fuse and emergency stop	Trip test	3 of 3 successful

A.9 Source Verification Audit

Table A9. Reference-audit record.

Reference group	DOI or source	audit status
Abelenda and Aiouache	10.3390/recycling8030046	DOI metadata matched
Bilal et al.	10.3390/recycling9050072	DOI metadata matched
Caceres et al.	10.1016/j.clwas.2023.100100	DOI metadata matched
Colorado et al.	10.1016/j.jmrt.2020.04.062	DOI metadata matched
Hidalgo-Carvajal et al.	10.3390/polym15173651	DOI metadata matched
Kassab et al.	10.3390/polym15193881	DOI metadata matched
Mishra et al.	10.1007/s10163-022-01588-2	DOI metadata matched
Rattan et al.	10.1016/j.ohx.2023.e00401	DOI metadata matched
Romani and Levi	10.3390/su16187966	DOI metadata matched
Sanchez et al.	10.1016/j.jclepro.2020.121602	DOI metadata matched
Shanmugam et al.	10.1007/s42824-020-00012-0	DOI metadata matched
Van De Voorde et al.	10.1016/j.addma.2021.102518	DOI metadata matched
United Nations Environment Programme	UNEP report page	Publisher page verified